IJBMS

Conjugated PNC-27 peptide/PEI-superparamagnetic iron oxide nanoparticles (SPIONs) as a double targeting agent for early cancer diagnosis: *In vitro* study

Reihaneh Rahmani [1, 2]**, Majid Darroudi** [3, 4]**, Mohsen Gharanfoli** [2, 5]**, Jamshidkhan Chamani** [6]**, Mehran Gholamin** [1, 7]*****, Maryam Hashemi** [8, 9]*****

[1] Department of Laboratory Sciences, School of Paramedical Sciences, Mashhad University of Medical Sciences, Mashhad, Iran
[2] Research Institute of Applied Sciences (ACECR), Shahid Beheshti University, Tehran, Iran
[3] Nuclear Medicine Research Center, Mashhad University of Medical Sciences, Mashhad, Iran
[4] Department of Medical Biotechnology and Nanotechnology, School of Medicine, Mashhad University of Medical Sciences, Mashhad, Iran
[5] Department of Cell and Molecular Biology, Faculty of Basic Sciences and Advanced Technologies in Biology, University of Science and Culture, Tehran, Iran
[6] Department of Biology, Faculty of Sciences, Mashhad Branch, Islamic Azad University, Mashhad, Iran
[7] Immunology Research Center, Mashhad University of Medical Sciences, Mashhad, Iran
[8] Department of Pharmaceutical Biotechnology, School of Pharmacy, Mashhad University of Medical Sciences, Mashhad, Iran
[9] Nanotechnology Research Center, Pharmaceutical Technology Institute, Mashhad University of Medical Sciences, Mashhad, Iran

ARTICLE INFO

ABSTRACT

Objective(s): Superparamagnetic iron oxide nanoparticles (SPIONs) have been considered promising non-invasive imaging tools in medicine. However, their high surface energy leads to NPs aggregation, while non-targeted SPIONs can cause cytotoxic effects on normal cells. In this work, we evaluated the *in vitro* potential of polyethyleneimine (PEI)-SPIONs targeted by PNC-27 peptide as a double targeting agent throughout early cancer diagnosis.

Materials and Methods: Initially, PEI was conjugated to PNC-27 with HDM-2-binding domain. Then, SPIONs were loaded into PEI-PNC-27 through the ligand exchange method. The physicochemical characteristics of the synthesized NPs were evaluated. The cytotoxicity and targeting efficiency were assayed against HT-29 and CT-26 cell lines along with NIH-3t3 as normal cells by MTT method and Prussian blue staining test, respectively.

Results: The mean diameter of synthesized carriers was obtained in the range of 86.6 – 116.1 nm with a positive charge. According to the cytotoxicity results, the binding and uptake abilities of the PNC-27 peptide by cancer cells were significantly higher than that of the NIH-3t3 cells. However, the results were indicative of the more toxic impacts of targeted synthesized NPs against CT-26 cancer cell line when being compared with HT-29 cells, which may be caused by the different cytotoxicity mechanisms of NPs. In addition, the targeted carriers and SPIONs were present inside and around the cells with HDM-2 expression along with only a few non-targeted vectors, while displaying no appearance throughout the normal cell.

Conclusion: The results indicated the efficiency of targeted PEI-coated SPIONs for cancer diagnostic applications.

Introduction

Cancer stands as a leading cause of morbidity and mortality in the world. However, early diagnosis of this disease can increase the chances of survival and efficiency of treatments. The current diagnostic imaging techniques applied in cancer clinical management include magnetic resonance imaging (MRI) and X-ray computed tomography (CT) (1), positron emission tomography (PET), and single-photon emission tomography (SPECT) (2, 3). However, these methods can only detect proliferated and metastasized cancer cells with significant changes. Recently, nanotechnology attracted the attention of many for performing the early detection of cancer mainly due to providing a large surface area to volume ratio that can be covered with cancer-targeting agents. As a promising non-invasive imaging method, magnetic NPs possess the properties of magnetic and NPs at the same time (4). Superparamagnetic iron oxide NPs

(SPIONs) are some of the most commonly used magnetic NPs with unique properties such as biocompatibility, simple synthesis, magnetic superchargers, and small size while offering the possibility of surface modification (5-8). The wide applications of this material can be observed in various therapeutic applications such as MRI, targeted delivery of drugs or genes, hyperthermia, and tissue engineering (9-11). Although SPIONs are sized in the range of 5–100 nm, their high surface energy typically leads to the aggregation of NPs. One of the approaches for reducing the intrinsic magnetism and stabilizing aqueous SPIONs is the coating of NPs with specific polymers such as poly (lactic-co-glycolic acid) (PLGA) (12), Polyethylene glycol (PEG) (13), Chitosan (14), and Polyethyleneimine (PEI) (15, 16). The complex of high cationic charge density of PEI with drugs or genes can improve their pharmacokinetic properties and cellular uptake. Recently, our group reported a novel green co-

---

*Corresponding authors: Mehran Gholamin. Department of Laboratory Sciences, School of Paramedical Sciences, Mashhad University of Medical Sciences, Mashhad, Iran; Immunology Research Center, Mashhad University of Medical Sciences, Mashhad, Iran. Email: GholaminM@mums.ac.ir; Maryam Hashemi. Departments of Pharmaceutical Biotechnology, School of Pharmacy, Mashhad University of Medical Sciences, Mashhad, Iran. Email: hashemim@mums.ac.ir

precipitation method for synthesis of SPIONs at laboratory temperature and air atmosphere with the application of a few chemical solutions, which proved to be much easier than the usual chemical co-precipitation method (17, 18).

In addition, we exerted quince seeds extract as a stabilizer agent to decrease the accumulation of SPIONs (17). Recently, targeted SPIONs were enhanced to identify specific cell-surface receptors on cancer cell types and reduce their cytotoxicity. As a protein receptor, HDM-2 is generally over-expressed on the surface of many cancer cells while having a minimal presence on the membranes of normal cell lines. Peptide PNC-27 with the self-identifying sequence of H-Pro-Pro-Leu-Ser-Gln-Glu-Thr-Phe-Ser-Asp-Leu-Trp-Lys-Leu-Leu contains the HDM-2-binding domain, which is located near the plasma membrane. The linking of the MRP segment (a transmembrane penetrating peptide) to the PNC-27 peptide induces pore-forming activity in the cell membrane and leads to cell necrosis (19). In this study, we evaluated the *in vitro* potential of targeted PEI-SPIONs by PNC-27 peptide without MRP domain as a double targeting agent to be considered for the early diagnosis of cancer.

Materials and Methods

Materials

Branched-Polyethylenimine (B-PEI~10 kDa) is a highly branched liquid water-soluble polyamine with high cationic charge density which was purchased from Sigma Aldrich (Germany), N-Succinimidyl 3-(-pyridine-2-thione). Propionate (SPDP) was obtained from Fluka (Buchs, Switzerland). PNC-27 peptide, Ac-CGGGPPLSQETFSDLWKLL, was acquired from Chinapeptides Co. (Shanghai, China) and >97% purified by HPLC and mass spectrographic methods. Iron Stain Kit (Prussian blue Stain, USA). All of the chemicals and solvents were of analytical grade and water was deionized before being utilized throughout the experiments.

Green synthesis of SPIONs

The SPIONs were synthesized in accordance with our previous report's description (17). Briefly, iron (II) chloride tetrahydrate and iron (III) chloride with a molar ratio of 2:1 were added to 150 ml of quince seeds extract and stirred continuously at 300 rpm at a temperature of 60 °C. After 30 min, the pH of the solution was adjusted to 11 by the usage of NaOH (0.20 M) solution. The obtained NPs were collected by a magnet and centrifuged (9,000 rpm, at 4 °C for 20 min), and the resultant was washed several times with water. Finally, the produced SPIONs were dried in an oven (70 °C) for 24 hr (Scheme 1).

Coated of SPIONs using B-PEI

The preparation of loaded SPIONs was done through a ligand-exchange method with the usage of B-PEI (20, 21). To state in detail, SPIONs (1.0 mg) were dispersed into B-PEI solution (10 mg in 1.0 ml of chloroform) by the utilization of a sonicating bath for 3 min. Then, the reaction mixture was stirred overnight at room temperature. Once the SPIONs-Loaded B-PEI was precipitated by the addition of 10 ml of hexane, the resultant was collected through centrifugation (8,000 rpm, at 20 °C for 20 min) and washed twice with hexane; then the product was vacuum-dried to remove the organic solvent. Subsequent to dispersing

Scheme 1. Schematic diagram of green synthesis of SPIONs by quince seed mucilage

the product into double-distilled water under sonication, it was filtered through a 220 nm membrane for removing the large aggregates and stored at -20 °C for the upcoming experiments. The amount of PEI in the final product was determined by means of 2,4,6-trinitrobenzene sulfonic acid (TNBS) assay as described previously (22).

Synthesize of 3-(2-pyridyldithiol) propionate modified B-PEI

B-PEI was conjugated to the hetero-bifunctional cross-linker N-succinimidyl 3-(-pyridine-2-thione) propionate (SPDP).

For this purpose, 0.50 ml of B-PEI stock 10 kDa (10.0 mg/ml in distilled water, pH= 7.2) was added to a 1.50 ml PBS buffer solution. Then, dissolved SPDP in DMSO (1.0 mg and 2.0 mg for 5 and 10% surface amine substitution, respectively) was appended drop wisely to B-PEI solution and stirred for 18 hr at room temperature to be purified through the application of dialysis tubing (Amicon, Beverly, MA, USA, molecular weight cut-off 3 kDa). Thereafter, the ultimate products (PEI-SPDP 5% and PEI-SPDP 10%) were stored at 4 °C. The degree of SPDP conjugation was determined by measuring the absorption of 3-(2-pyridyldithiol) propionate (PDP) and utilizing the excess of DTT at 343 nm with the molar absorptivity of 8.08×10^3 M^{-1} cm^{-1}.

Conjugation of PNC-27 peptide to PEI-SPDP

Peptide conjugation was performed according to the disulfide bond of PEI-SPDP and PNC-27; one mole of SPDP linker must react with one mole of a peptide (23). PEI-SPDP (5.0 mg of PEI) containing 1.25 μmol and 2.7 μmol of SPDP was mixed with 2.5 mg or 5.5 mg of peptide (two-fold excess) for 5% and 10% substitution, respectively; then, they were incubated for 4 hr at room temperature. To measure the amount of peptide conjugation, the absorption of released thiopyridone was determined at 343 nm. As the last step, the unreacted peptides were removed by dialysis against distilled water through centrifugation, which involved the application of an Amicon® ultra centrifugal filter (6,000 rpm, at 4 °C for 15 min). The purified products (PEI-SPDP %5-PNC-27 and PEI-SPDP %10-PNC-27) were kept frozen at -20 °C until further usage.

Coated of SPIONs by PEI-SPDP-PNC-27

According to the mentioned ligand exchange method, PEI-SPDP 5%-PNC-27 (containing 1.0 mg of PEI and 225 μl of PNC-27) was added to 1.0 mg/ml of SPION solution. Also, PEI-SPDP 10%-PNC-27 (containing 1.5 mg of PEI and 270 μl of PNC-27) was added to 1.5 mg/ml of SPION solution. Then, both of the mixtures were stirred at room temperature for 3 hr by the use of a magnet to have the

Rahmani et al.
IJ|BMS
PNC-27 peptide/PEI-SPIONs for early cancer diagnosis

reaction mixture stirred overnight at room temperature.

The loaded SPIONs in PEI-SPDP-PNC-27 were precipitated by adding 10 ml of hexane, which were then collected through centrifugation (6,000 rpm, at 4 °C for 15 min). All of the products were washed twice with hexane and vacuum-dried to remove the organic solvent; in this way, they were dispersed into double-distilled water under sonication and filtered through a 220 nm membrane (to remove large aggregates and unreacted solvents), and after that to be kept at -20 °C for further usage. The amount of PEI in the final product was determined by the means of 2,4,6-trinitrobenzene sulfonic acid (TNBS) assay as described previously (22). The abbreviations of synthesized formulations are presented in Table 1.

Physicochemical characterization of synthesized NPs
Particle size and zeta potential measurements

The hydrodynamic diameters and zeta potential of SPIONs and obtained nano-vectors were measured through Dynamic Light Scattering and Laser Doppler Velocimetry, respectively, by application of a Malvern Nano ZS instrument and DTS software (Malvern Nano ZS, UK). For this purpose, 1.0 mg of synthesized NPs was suspended in 1.0 ml of double-distilled water (24) and sonicated for 20 min to turn into a homogeneous suspension. The gathered data represent the average ±standard deviations, while the analysis was performed in triplicate and all of the measurements were recorded at 25 °C.

Morphological studies

The morphological study of SPIONs, PS 5%-PNC@SPI, and PS 10%-PNC@SPI was characterized by utilization of a Field Emission Scanning Electron Microscope (FE-SEM; TESCAN Mira3, Czech Republic), which operated at 5.0 kV accelerating voltage and 1.5 cm working distance between the samples and detector.

Determination of iron concentration

Atomic Absorption Spectroscopy (AAS) (Varian, 240FS FLAME AA Spectrometer, USA) was used to determine the concentration of Fe_3O_4 NPs in P@SPI, PS 5%-PNC@SPI, and PS 10%-PNC@SPI (25). Initially, a calibration diagram was obtained using standard solutions within the concentration range of 1.25, 2.50, 5.0, and 10.0 µg/ml. Then, the absorption of the unknown solution was measured and the concentration of the unknown element was determined

from the standard curve.

Evaluation of integrity of PNC-27 peptide

The performance of Tricine-Sodium Dodecyl Sulfate Polyacrylamide Gel Electrophoresis (SDS PAGE) was considered to confirm the conjugation of PNC-27 peptide to PEI, which was in accordance with Laemmli with some modifications (26). Briefly, PS 5%-PNC@SPI and PS 10%-PNC@SPI were analyzed by the usage of 15.0 % acrylamide separation gels with a 5.0 % stacking gel under reducing conditions. Samples were diluted at a 1:1 ratio with sample buffer and boiled at 95 °C (27). Subsequent to the loading of samples and electrophoresis (80 v, 30 mA for 30 min), the gels were stained with Coomassie brilliant blue 0.1% w/v.

In vitro cellular study
Cell culture

Two cancer cell lines that overexpress HDM-2, including HT-29 cell line (human colorectal adenocarcinoma cell line) and CT-26 cell line (murine colorectal carcinoma cell line)), as positive cells were procured from ATCC along with NIH-3t3 (mouse embryonic fibroblast cell line) as a negative cell to function like the normal cells. The HT-29 and CT-26 cell lines were cultured in RPMI (Roswell Park Memorial Institute 1640), while the NIH-3t3 cell line was grown in DMEM (Dulbecco's Modified Eagle's medium from Biosera, UK).

Meanwhile, both of the culture mediums were supplemented with 10.0% fetal bovine serum (VWR, Visalia, CA, USA) and 1.0% penicillin-streptomycin (Sigma, St. Louis, MO, USA). The cells were maintained in an incubator at 37 °C with a humidified atmosphere of 5.0% CO_2. The cells that were in the exponential growth phase were exerted to perform all of the experiments.

Cytotoxicity assay

A comparison experiment was done to determine the targeting and cytotoxicity qualities of SPIONs, PEI, and nano-vectors containing both SPIONs and PEI, which was executed through the usage of 3-(4,5-Dimethylthiazol-2-yl)-2, 5-diphenyltetrazolium bromide (MTT assay) (28). The cell lines (HT-29, CT-26, and NIH-3t3) were seeded in a 96-well plate at the density of 1×10^4 cells/well in the assigned medium and incubated at 37 °C. After 24 hr, the cells were treated with a serial concentration of SPIONs NPs (0.012 to 3.2 µg/ml), PEI (0.15 to 80.0 µg/ml), P@SPI, PS 5%-PNC@SPI, and PS 10%-PNC@SPI (containing 0.02 to 0.8 µg/ml SPIONs) to be incubated for 24 hr. Subsequently, the medium was aspirated to have the wells cleansed with PBS and the procedure was followed by appending 200.0 µl of fresh medium to each well. Then, 10.0 µl of MTT (5.0 mg/ml in PBS) solution was added into each well and after 4 hr of incubation, the total medium was replaced with DMSO (100 µl). The absorbance of samples was recorded at 570 nm through the application of a BioRad microplate reader with a reference wavelength of 630 nm. The cell viability (%) relative to control wells containing cell culture medium without treatment was calculated using A_{test} / $A_{control}$ ×100.

Qualitative binding study

The existing intracellular iron can be detected through the method of Perl's Prussian Blue (PB) staining (29). Briefly, CT-26 and HT-29 cancer cells were seeded in six-well plates

Table 1. List of abbreviations of synthesized nano-vectors

Formulations	Abbreviated name of vectors
PEI-SPIONS	P@SPI
PEI-SPDP 5%	PS 5%
PEI-SPDP 10 %	PS 10%
PEI-SPDP 5%-PNC27	PS 5%-PNC
PEI-SPDP 10%-PNC27	PS 10%-PNC
PEI-SPDP 5%-PNC27@SPIONs	PS 5%-PNC@SPI
PEI-SPDP 10%-PNC27@SPIONs (PEI-SPDP-PNC27@SPIONs)	PS 10%-PNC@SPI (PS-PNC@SPI)

PEI: Polyethyleneimine; SPDP: N-Succinimidyl 3-(-pyridine-2-thione) Propionate; SPION: Superparamagnetic iron oxide NPs

at the density of 2.0×10^5 cells/well and incubated overnight.

Then, the cells were washed and exposed to the samples of SPIONs (2.0 µg/ml), P@SPI, PS 5%-PNC@SPI, and PS 10%-PNC@SPI containing 3.4, 3.2, and 2.4 µg/ml SPIONs, respectively to be incubated afterward for 4 hr. Then, the cells were washed three times with cold PBS and fixed with 4.0% v/v formaldehyde for 10 min to be incubated for 20 min with 4.0% potassium ferrocyanide and 4.0% HCl solution. Subsequently, the cells were cleaned again with PBS to be stained with a nuclear fast red solution for 30 min. Finally, the cells were washed with DI water and rapidly dehydrated through alcohol to go under surveillance by the usage of a Zeiss Axiovert 40 CFL microscope. As the control sample, NIH-3t3 cells (normal cell line) were treated with a similar procedure.

Statistical analysis

All of the statistical analyses were performed through the utilization of Graph Pad Prism 6 Software. Results were expressed as mean±standard deviation (SD).

Results

The focus of this study was centered on PNC-27 peptide conjugated PEI-SPIONs NPs as a double targeting agent for the early diagnosis of cancer. The schematic representation of the synthesized PS-PNC@SPI nano-vector is presented in Figure 1.

Preparation of peptide-conjugated PEI

To develop the targeted SPIONs, PEI was initially activated with SPDP as displayed in Figure 1 (a). Accordingly, about 77% and 86% of primary amine contents of PS 5% and PS 10% were modified with SPDP, respectively. Then, the peptide was added to PEI-DTP in the assigned concentrations to achieve the conjugation of 5 and 10% of primary amines with peptides (Figure 1 (b)).

The amount of released 2-thiopyridone in the presence of peptide indicated that the yield of the reaction was about 90% for the two formulations. The concentration of PEI in final products in conformity to the TNBS test is provided
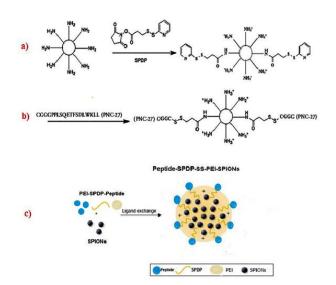
Table 2. Concentration of PEI polymer in synthesized products

Sample	P@SPI	PS 5%-PNC	PS 10%-PNC	PS 5%-PNC@SPI	PS 10%-PNC@SPI
PEI (µg/100 µl)	65.81	72.30	11.38	30.54	68.61

PEI: Polyethyleneimine; P@SPI: PEI-SPION; PS 5%-PNC: PEI-SPDP-5% Peptide; PS 10%-PNC: PEI-SPDP-10% Peptide; PS 5%-PNC@SPI: PEI-SPDP-5% Peptide-SPION; PS 10% -P NC@SPI: PEI-SPDP-10% Peptide-SPION

Table 3. Size, PDI, and zeta potential of obtained NPs by DLS

NPs	Z_{AVE} (nm) ± SD	PDI	ξ-potentials(mV) ± SD
SPIONs	145.5 ± 6.2	0.16	62.9 ± 2.1
P@SPI	133.8 ± 3.6	0.11	61.7 ± 1.3
PS 5%-PNC@SPI	102.1 ± 2.1	0.11	30.2 ± 3.2
PS 10%-PNC@SPI	96.2 ± 2.3	0.38	25.1 ± 3.4

PDI: Particle size dispersion; DLS: Dynamic Light Scattering

in Table 2.

Characterization of synthesized NPs

The mean diameter of synthesized SPIONs was obtained in the range of 86.6–116.1 nm with a positive charge through application of the DLS method. According to the displayed size (Z-average) and zeta potential of all the NPs in Table 3, the loading of SPIONs into B-PEI or PS-PNC-27 resulted in a significant decrease in these values. However, in this study, all of the obtained NPs contained a suitable size and adequate positive charge for attaching to the surface of cells.

We evaluated the morphology of obtained NPs through the employment of FE-SEM, which was synthesized, and the results were illustrated in Figure 2. Following the captured FE-SEM images, the shape of NPs was detected to be spherical as displayed in Figure 2 (a) within the size range of 20–50 nm which can be seen in Figure 2 (b). The obtained outcomes confirmed the smooth morphology and particle size of the nanoparticle's distribution plot of PS-PNC@SPI, which was calculated to be approximately 32.50
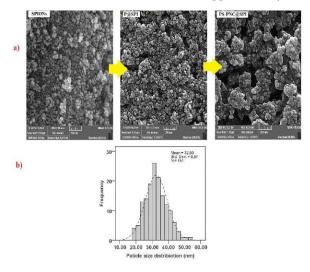

Figure 1. Steps of creating synthesized nano-vectors; Formation of the PEI-B-SS-SPDP compound (a), Conjugation of PNC27 peptide loading to PS (b), Loading of SPIONs in PS-PNC conjugate by ligand exchange method, and creation of PS-PNC@SPI nano-vector (c)
PS: PEI-SPDP; PS-PNC: PEI-SPDP-Peptide; PS-PNC@SPI: PEI-SPDP-Peptide-SPION

Figure 2. (a) Morphologies of particles. FE-SEM images of SPIONs, P@ SPI, and PS-PNC@SPI nano-vector. (b) Obtained particle size of PS-PNC@SPI by ImageJ software
P@ SPI: PEI-SPION; PS-PNC@SPI: PEI-SPDP-Peptide-SPION

Table 4. Amount of iron in each product by atomic absorption spectroscopy (AAS)

NPs	Fe (µg/ml)
P@SPI	56 ± 5.1
PS 5%-PNC@SPI	64 ± 3.0
PS 10%-PNC@SPI	80 ± 2.4

P@SPI: PEI-SPION; PS 5%-PNC@SPI: PEI-SPDP-5% Peptide-SPION; PS 10% -PNC@SPI: PEI-SPDP-10% Peptide-SPION

(Figure 2 (b)).

Iron content determination

The existing iron concentration in final products was determined by atomic absorption spectrophotometry (AAS) at 248 nm (SpectrAA-10 plus, Varian, France) (Table 4).

A calibration curve was obtained by treating an acidic solution of $FeCl_3$ (1.0 g/l) in similar conditions.

Tricine-SDS page

The tricine-SDS-PAGE test was performed to confirm the presence of peptide in PS-PNC@SPI targeted nano-vector and have it compared with non-targeted P@SPI nano-vector. As exhibited in Figure 3, the presence of the PNC-27 peptide in the targeted nano-vector confirmed the binding of the PNC-27 identifier peptide to the B-PEI polymer.

In vitro cytotoxicity assay

The cytotoxicity of SPIONs, B-PEI-10 KDa, P@SPI, PS 5%-PNC@SPI, and PS 10%-PNC@SPI nano-vectors were evaluated against positive cells, HT-29 and CT-26, and also negative cell, NIH-3t3, by the means of MTT assay. In conformity to Figure 4, the highest survival rate against SPIONs was observed in HT-29 cell lines (more than 80%) and the highest effect of toxicity was observed in CT-26 cell line after 24 hr. The cell viability percentage was higher than 60% in three cell lines against all of the studied concentrations of SPIONs.

The toxicity results of B-PEI 10 Ka indicated a survival rate of higher than 60% at concentrations up to 20 µg/ml for NIH-3T3 and HT-29 cell lines (Figure 5). However, the
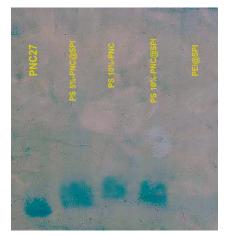

Figure 4. Evaluation of the cytotoxicity effect of SPIONs on HT-29 and CT-26 cancer cell lines and NIH-3t3 normal cell line by MTT assay after 24 hr (Mean±SD; n=5)

highest toxicity of PEI polymer was obtained in the case of CT-26 cancer cell line, which suggests the higher sensitivity of mouse clone cancer cells.

In this section, we evaluated the cytotoxicity effect of synthesized NPs containing 0.025–0.8 µg/ml of SPIONs. The amount of PEI polymer (determined by TNBS test) and Fe in NPs that contained 0.8 µg/ml of SPIONs (the highest exerted concentration of SPIONs) are demonstrated in Table 5.

According to Figure 6, SPIONs-loaded PEI induced the lowest toxicity in normal cells and also caused 50% of survival in concentrations up to 0.4 µg/ml for the HT-29 cell line. However, the highest toxicity was expected to be observed throughout the CT-26 cell line, since the application of concentrations up to 0.1 µg/ml is typically required to achieve a cell survival of more than 50% in the case of non-targeted P@SPI nano-vector.

The cytotoxicity results of targeted NPs indicated more than 50% of cell survival for both cases of NIH-3t3 normal and HT-29 cancer cell lines throughout all of the experimented concentrations (Figure 7). Furthermore, PS 10%-PNC@SPI displayed higher cytotoxicity than PS 5%-PNC@SP. In addition, synthesized carriers showed a significant toxicity effect against CT-26 cell line at a

Figure 3. Coomassie-stained SDS-PAGE photograms of PNC27 peptide in PS 5% -PNC@SPI and PS 10%-PNC@SPI
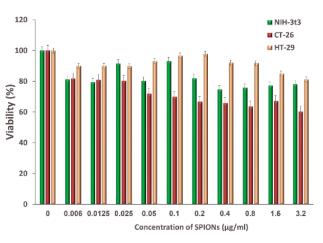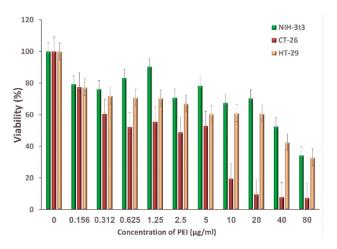PS 5%-PNC@SPI: PEI-SPDP-5% Peptide-SPION; PS 10% -PNC@SPI: PEI-SPDP-10% Peptide-SPION

Figure 5. Evaluation of cytotoxicity effect of B-PEI 10 KDa polymer on HT-29 and CT-26 cancer cell lines and NIH-3t3 normal cell line by MTT assay after 24 hr (Mean±SD; n=5)

Table 5. Amount of SPIONs and PEI polymer in nano-vectors at the highest concentration of SPIONs

Sample	Fe (μg/ml)	SPIONs (μg/ml)	Amount of sample	Volume of culture medium	PEI (μg/ml)
P@SPI	56 ± 5.1	0.8	14.2 μl NPs	986 μl	9.3
PS 5-%PNC@SPI	64 ± 3.0	0.8	12.9 μl NPs	987 μl	3.9
PS - %10P NC@SPI	80 ± 2.4	0.8	10 μl NPs	990 μl	6.8

P@ SPI: PEI-SPION; PS 5%-PNC@SPI: PEI-SPDP-5% Peptide-SPION; PS 10%-PNC@SPI: PEI-SPDP-10% Peptide-SPION; SPION: Superparamagnetic iron oxide NPs; PEI: Polyethyleneimine
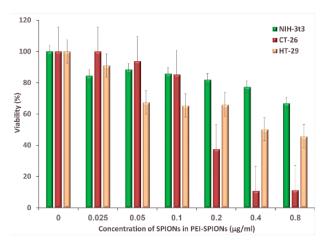

Figure 6. Evaluation of cytotoxicity effect of non-targeted P@SPI nano-vector on HT-29 and CT-26 cancer cell lines and NIH-3t3 normal cell line by MTT assay after 24 hr (Mean±SD; n=5)

concentration of more than 0.2 μg/ml of SPIONs.

Prussian blue staining

Prussian Blue staining (PB) was used to confirm the uptake of SPIONs in cells (30). For this purpose, the cells were treated with non-targeted and targeted NPs that contained 0.2 and 0.1 μg/ml of SPIONs (non-toxic concentrations), respectively, for 2 hr.

As exhibited in Figure 8, Dyed SPIONs formed around the cancer cell membranes in targeted nano-vectors, which confirms the binding of peptide PNC-27. Also, it confirmed
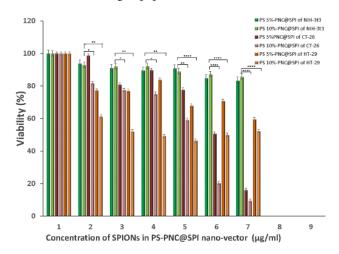

Figure 7. Evaluation of cytotoxicity effect of PS 5%-PNC@SPI and PS 10%-PNC@SPI nano-vector on HT-29 and CT-26 cancer cell lines and NIH-3t3 normal cell line by MTT assay after 24 hr (Mean±SD; n=5)
P@SPI: PEI-SPION; PS 5%-PNC@SPI: PEI-SPDP-5% Peptide-SPION; PS 10% -P NC@SPI: PEI-SPDP-10% Peptide-SPION
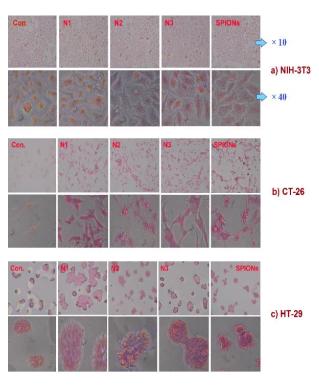

Figure 8. Confirmation of SPIONs and their derivatives around the cell membrane in CT-26 (b) and HT-29 (c) cancer cell lines relative to the normal NIH-3T3 (a) cell. (Control cells (Con.), Non-targeted nano-vector P@SPI (N1), targeted nano-vectors PS 5%-PNC@SPI (N2) and PS 10%-PNC@SPI (N3), and SPIONs)
P@ SPI: PEI-SPION; PS 5%-PNC@SPI: PEI-SPDP-5% Peptide-SPION; PS 10%-PNC@SPI: PEI-SPDP-10% Peptide-SPION

the binding of PS 5%-PNC@SPI and PS 10%-PNC@SPI targeted nano-vectors to the surface of cancer cells by HDM-2 marker. This test was performed against normal NIH-3T3 cells as well. The absence of SPIONs around these cells confirmed the binding of targeted PNC-27 to the HDM-2 receptor on the surface of human and mouse clone cancer cells.

Discussion

SPIONs stand as potential candidates for cancer diagnosis due to their being biodegradable, biocompatible, and readily endocytosed by a variety of different cell properties. However, the gathered data are indicative of non-targeted SPIONs cytotoxicity towards normal cells. Furthermore, the surface functionalization of SPIONs through various bioligands can increase its specificity to tumor targeting. *Vu-Quang et al.* developed an imaging nano-system based on SPIONs that was coated with Pluronic F127-Folateto target folate receptor-expressing cancer cells. According to their *in*

vitro results and *in vivo* MRI images, these stable NPs could preferentially target oral squamous cancer (KB) cells by folate receptors expressed on their membranes and through the enhanced negative contrast in tumor-bearing mice (31). In another study, Hu *et al.* reported the high efficiency of arginine-glycine-aspartic acid (RGD) peptide-targeted iron oxide (Fe_3O_4) NPs with ultrahigh relaxivity for *in vivo* MR imaging. In this study, Fe_3O_4 NPs were coated with PEI by the application of a mild reduction method, which was followed by conjugation with fluorescein isothiocyanate (FI), PEGylated RGD (PEG-RGD), and lastly acetylation of the remaining PEI surface amines.

The RGD-mediated targeting specificity of NPs to αvβ3 integrin-overexpressing cancer cells was also discovered. It was indicated that these targeted NPs could efficiently target U87MG cells overexpressing αvβ3 integrin with ultrahigh R_2 relaxivity for MR imaging of tumors (32). In conformity to further examinations, surface functionalization of SPIONs by different bioligands such as dextran, hybrid chitosan-dextran, and protein Hsp70 can increase the specificity of brain tumor targeting (33-35). In addition, SPIONs were conjugated with recombinant human epidermal growth factor (SPION-EGF), and their efficiency in performing the MIR of malignant brain tumors overexpressing EGF receptors was evaluated. The results revealed that these targeted magnetic NPs are capable of displaying high MR contrast in the C6 rat glioma model (36). Recent studies indicated the overexpression of HDM-2 protein on the surface of most cancer cells such as breast, colon, glioblastoma, prostate, and pancreatic cancers, which also prompts the transmembrane pore arrangement in malignancy without causing any impact on normal cells (37, 38). PNC-27 is a membrane-active peptide that contains a corresponding HDM-2-binding domain to the residues of p53 and a transmembrane-penetrating domain (37). In recent years, several studies were focused on the functionality of PNC-27 peptide as a targeting or anticancer agent (37, 39). Darban *et al.* evaluated the targeting ability of conjugated Doxil (a stealth liposomal formulation of doxorubicin) with PNC-27 peptide in CT-26 colon carcinoma cells (HDM2 positive). Their outcomes were suggestive of an exceptionally significant improvement in the restricting and uptake of targeted formulations, which is in contrast with the results of non-targeted Doxil in CT-26 tumor-bearing mice (40). Mokhtarzadeh *et al.* studied the efficiency of PEI 10 kDa and alkylcarboxylated PEI 10 kDa targeted with PNC-27 and PNC-28 peptides involved in interactions with HDM-2 situated for delivering GFP-containing Sure Silencing shRNA plasmid into MCF-7 cells. According to the gathered results, the conjugation of PNC peptides can enhance the gene delivery efficiency of both PEI and alkylated PEI with high-targeted activity exclusively in cancer cells (41). Notwithstanding, perceptions were predictable with the outcomes from a 2D NMR concentrating on the design of PNC-27 appearance that this peptide adopts a strongly amphipathic alpha-helix-loop-alpha-helix structure (19, 42), In our previous work, we performed the synthesis of SPIONs through an eco-friendly and green method by the usage of Quince seeds (*Cydonia oblonga* Miller*)* extract as a bio-stabilizer. That experiment resulted in achieving SPIONs with a spherical shape and a size of less than 50 nm. In addition, *in vitro* cytotoxicity studies indicated the low toxicity effect of the obtained

product against A549 cells in concentrations lower than 100 µg/ml (17). In this study, peptide-identifying sequences of PNC-27 were used to target overexpressed HDM-2 on cancer cells. Therefore, we evaluated the *in vitro* functionality of PNC-27 peptide conjugated PEI-SPIONs as a double targeting agent for the early diagnosis of cancer. As a strong cationic polymer, PEI was exerted to improve the stability of SPIONs. In this regard, PEI with a molecular weight of 10 KD was selected due to its lower cytotoxicity and higher efficiency when compared with the higher and lower Mw of PEI, respectively. In different studies, PEI was used along with SPIONs as a targeted drug or gene delivery system throughout the diagnosis and treatment of cancer (43-45). The diameter and surface charge of NPs affect their uptake, stability, and transfer efficiency (46). Additionally, the results of the current study indicated that the loading of SPIONs into PEI or PS-PNC-27 caused a size reduction, which may be due to the active surface of naked SPION NPs that leads to their tendency for forming aggregations with each other. However, the stabilization of SPIONs that was accompanied by PEI decreased the aggregation percentage of NPs. The lower surface charge of PEI and PNC-peptide (47) compared with SPION NPs may be the reason for the reduced zeta potential of coated SPIONs with PEI or PEI-PNC-27. In the next step, the cytotoxicity of the obtained products was examined by being applied to cancer cells (HT-29 and CT-26).

As exhibited in Figure 7, the binding and uptake abilities of PNC-27 by HT-29 and CT-26 cells were significantly higher than those of the NIH-3t3 cells due to the high-level expression of HDM2 in HT-29 and CT-26 cell lines resulting in the high uptake of the nanocomplex by the receptor into the cells. Furthermore, the results were indicative of the more toxic impacts of targeted synthesized NPs against the CT-26 cancer cell line when being compared with HT-29 cells, which may be caused by the different cytotoxicity mechanisms of NPs in varying cell lines. Also, PS 5%-PNC@SPI displayed lower cytotoxicity than PS 10%-PNC@SPI in the positive cell lines. To confirm the uptake of NPs in cells, Prussian blue (PB) was performed as a staining method, since it provides data on the accumulation of SPIONs or iron in cells by forming a complex with potassium ferricyanide. According to observations, SPIONs appeared in blue while cell bodies were colored in pink. As it can be perceived more specifically in Figure 8, the targeted nano-vectors (PS 5%-PNC@SPI and PS 10%-PNC@SPI) and SPIONs were present inside and around the cells with HDM-2 expression (HT-29 and CT-26) along with only a few non-targeted nano-vectors (P@SPI), while displaying zero appearance throughout the normal cell (NIH-3t3). Therefore, the appearance of iron oxide NPs around the cells can suggest the potential application of PS-PNC@SPI in molecular imaging and drug delivery, as well as the targeted identification of cancer cells.

Conclusion

In this work, we evaluated the *in vitro* potential of polyethyleneimine-superparamagnetic iron NPs (PEI-SPIONs) targeted by PNC-27 as a double targeting agent throughout the early cancer diagnosis. The results of the cytotoxicity study indicated that the binding and uptake abilities of PNC-27 by HT-29 and CT-26 cells were significantly higher than those of the NIH-3t3 cells due to

the high-level expression of HDM2 in HT-29 and CT-26 cell lines. Therefore, this targeting system may offer a novel approach to cancer diagnosis by reducing the inducement of side effects on normal cells. Moreover, the performed *in vitro* studies with the usage of PB as a staining method revealed significant improvements in binding targeted nano-vectors in HDM-2-overexpressing cancer cells when being compared with non-targeted nano-vector (P@SPI). In this system, the PNC-27 sequence can be exerted for targeting HDM-2 on the surface of cancer cells for an efficient diagnosis and also used for biocomplexity purposes. Overall, the obtained results confidently suggest the potential of PNC-27 peptides for serving as an efficient targeting agent for most cancer cells, as well as recommending the promising stand of targeted nano-vectors as targeted agents for diagnostic applications.

Acknowledgment

Authors' Contributions

RR, MD, MGho, and MH designed the experiments; RR performed experiments and collected data; RR, MD, MGha, JC, and MH discussed the results and strategy; MGho and MH supervised, directed, and managed the study; RR, MD, and MH approved the final version to be published.

Conflicts of Interest

Authors declare no conflicts of interest. The authors have no other relevant affiliations or financial involvement with any organization or entity with a financial interest in or financial conflict with the subject matter or materials discussed in the manuscript apart from those disclosed.

References

1. Gowtham P, Haribabu V, Prabhu AD, Pallavi P, Girigoswami K, Girigoswami A. Impact of nanovectors in multimodal medical imaging. Nanomed J 2022; 9: 107-130.
2. Zhang Y, Li M, Gao X, Chen Y, Liu T. Nanotechnology in cancer diagnosis: progress, challenges and opportunities. J Hematol Oncol 2019; 12:1-13.
3. Bakhtiari-Asl F, Divband B, Mesbahi A, Gharehaghaji N. Bimodal magnetic resonance imaging-computed tomography nanoprobes: A Review. Nanomed J 2020; 7: 1-12.
4. Lu C, Han L, Wang J, Wan J, Song G, Rao J. Engineering of magnetic nanoparticles as magnetic particle imaging tracers. Chem Soc Rev 2021; 50: 8102-8146.
5. Tomitaka A, Hirukawa A, Yamada T, Morishita S, Takemura Y. Biocompatibility of various ferrite nanoparticles evaluated by *in vitro* cytotoxicity assays using HeLa cells. J Magn Magn Mater 2009; 321: 1482-1484.
6. Subbiahdoss G, Sharifi S, Grijpma DW, Laurent S, van der Mei HC, Mahmoudi M, *et al*. Magnetic targeting of surface-modified superparamagnetic iron oxide nanoparticles yields antibacterial efficacy against biofilms of gentamicin-resistant staphylococci. Acta Biomater 2012; 8: 2047-2055.
7. Weissig V, Guzman-Villanueva D. Nanopharmaceuticals (part 2): Products in the pipeline. Int J Nanomedicine 2015; 10: 1245-1257.
8. Revia RA, Zhang M. Magnetite nanoparticles for cancer diagnosis, treatment, and treatment monitoring: Recent advances. Materials Today 2016; 19: 157-168.
9. Ito A, Shinkai M, Honda H, Kobayashi T. Medical application of functionalized magnetic nanoparticles. J Biosci Bioeng 2005; 100: 1-11.
10. Liu F, Le W, Mei T, Wang T, Chen L, Lei Y, *et al*. *In vitro* and *in vivo* targeting imaging of pancreatic cancer using a $Fe_3O_4@SiO_2$ nanoprobe modified with anti-mesothelin antibody. Int J Nanomed 2016; 11: 2195-2207.
11. Hajesmaeelzadeh F, Shanehsazzadeh S, Grüttner C, Daha FJ, Oghabian MA. Effect of coating thickness of iron oxide nanoparticles on their relaxivity in the MRI. Iran J Basic Med Sci 2016; 19: 166-177.
12. Mosafer J, Abnous K, Tafaghodi M, Mokhtarzadeh A, Ramezani M. *In vitro* and *in vivo* evaluation of anti-nucleolin-targeted magnetic PLGA nanoparticles loaded with doxorubicin as a theranostic agent for enhanced targeted cancer imaging and therapy. Eur J Pharm Biopharm 2017; 113: 60-74.
13. Almaki JH, Nasiri R, Idris A, Majid FAA, Salouti M, Wong TS, *et al*. Synthesis, characterization and *in vitro* evaluation of exquisite targeting SPIONs–PEG–HER in HER2+ human breast cancer cells. Nanotechnology 2016; 27: 105601.
14. Zia A, Rezaei Aghdam H, Saffari M, Farzaneh J, Pirali Hamedani M, Ebrahimi SES, *et al*. Novel chitosan-quinic acid nanoparticles labeled with m99 technetium for breast cancer imaging. Nanomed J 2022; 9: 231-240.
15. Mokhtarzadeh A, Parhiz H, Hashemi M, Ayatollahi S, Abnous K, Ramezani M. Targeted gene delivery to MCF-7 cells using peptide-conjugated polyethylenimine. AAPS Pharm Sci Tech 2015; 16: 1025-1032.
16. Parhiz H, Hashemi M, Hatefi A, Shier WT, Farzad SA, Ramezani M. Molecular weight-dependent genetic information transfer with disulfide-linked polyethylenimine-based nonviral vectors. J Biomater Appl 2013; 28: 112-124.
17. Rahmani R, Gharanfoli M, Gholamin M, Darroudi M, Chamani J, Sadri K. Green synthesis of 99mTc-labeled-Fe_3O_4 nanoparticles using Quince seeds extract and evaluation of their cytotoxicity and biodistribution in rats. J Mol Struct 2019; 1196: 394-402.
18. Rahmani R, Gharanfoli M, Gholamin M, Darroudi M, Chamani J, Sadri K, *et al*. Plant-mediated synthesis of superparamagnetic iron oxide nanoparticles (SPIONs) using Aloe vera and flaxseed extracts and evaluation of their cellular toxicities. Ceramics International 2020; 46: 3051-3058.
19. Sarafraz-Yazdi E, Bowne WB, Adler V, Sookraj KA, Wu V, Shteyler V, *et al*. Anticancer peptide PNC-27 adopts an HDM-2-binding conformation and kills cancer cells by binding to HDM-2 in their membranes. Proc Natl Acad Sci 2010; 107: 1918-1923.
20. Tromsdorf UI, Bigall NC, Kaul MG, Bruns OT, Nikolic MS, Mollwitz B, *et al*. Size and surface effects on the MRI relaxivity of manganese ferrite nanoparticle contrast agents. Nano lett 2007; 7: 2422-2427.
21. Luo Y, Yang J, Li J, Yu Z, Zhang G, Shi X, *et al*. Facile synthesis and functionalization of manganese oxide nanoparticles for targeted T1-weighted tumor MR imaging. Colloids Surf. B: Biointerfaces 2015; 136: 506-513.
22. Snyder SL, Sobocinski PZ. An improved 2, 4, 6-trinitrobenzenesulfonic acid method for the determination of amines. Anal Biochem 1975; 64: 284-288.
23. Meyer M, Philipp A, Oskuee R, Schmidt C, Wagner E. Breathing life into polycations: functionalization with pH-responsive endosomolytic peptides and polyethylene glycol enables siRNA delivery. ACS Symp Ser Am Chem Soc 2008; 130: 3272-3273.
24. Gollwitzer C, Bartczak D, Goenaga-Infante H, Kestens V, Krumrey M, Minelli C, *et al*. A comparison of techniques for size measurement of nanoparticles in cell culture medium. Anal Methods 2016; 8: 5272-5282.
25. Munnier E, Cohen-Jonathan S, Hervé K, Linassier C, Soucé M, Dubois P, *et al*. Doxorubicin delivered to MCF-7 cancer cells by superparamagnetic iron oxide nanoparticles: effects on subcellular distribution and cytotoxicity. J Nanoparticle Res 2011; 13: 959-971.
26. Laemmli UK. Cleavage of structural proteins during the assembly of the head of bacteriophage T4. Nature 1970; 227: 680-685.
27. Silva JM, Zupancic E, Vandermeulen G, Oliveira VG, Salgado A, Videira M, *et al*. *In vivo* delivery of peptides and Toll-like receptor ligands by mannose-functionalized polymeric

nanoparticles induces prophylactic and therapeutic anti-tumor immune responses in a melanoma model. J Control Release 2015 28; 198: 91-103.

28. Alibolandi M, Ramezani M, Abnous K, Sadeghi F, Atyabi F, Asouri M, *et al. In vitro* and *in vivo* evaluation of therapy targeting epithelial-cell adhesion-molecule aptamers for non-small cell lung cancer. J Control Release 2015; 209: 88-100.

29. Alvarez M, Quezada C, Navarro C, Molina A, Bouvet P, Krauskopf M, *et al.* An increased expression of nucleolin is associated with a physiological nucleolar segregation. Biochem Biophys Res Commun 2003; 301:152-158.

30. Gholami L, Oskuee RK, Tafaghodi M, Farkhani AR, Darroudi M. Green facile synthesis of low-toxic superparamagnetic iron oxide nanoparticles (SPIONs) and their cytotoxicity effects toward Neuro2A and HUVEC cell lines. Ceram Int 2018; 44: 9263-9268.

31. Vu-Quang H, Vinding MS, Nielsen T, Ullisch MG, Nielsen NC, Nguyen D-T, *et al.* Pluronic F127-folate coated super paramagenic iron oxide nanoparticles as contrast agent for cancer diagnosis in magnetic resonance imaging. Polymers 2019; 11: 743-757.

32. Hu Y, Li J, Yang J, Wei P, Luo Y, Ding L, *et al.* Facile synthesis of RGD peptide-modified iron oxide nanoparticles with ultrahigh relaxivity for targeted MR imaging of tumors. Biomater Sci 2015; 3:721-732.

33. Wankhede M, Bouras A, Kaluzova M, Hadjipanayis CG. Magnetic nanoparticles: an emerging technology for malignant brain tumor imaging and therapy. Expert Rev Clin Pharmacol 2012; 5: 173-186.

34. Shevtsov M, Nikolaev B, Marchenko Y, Yakovleva L, Skvortsov N, Mazur A, *et al.* Targeting experimental orthotopic glioblastoma with chitosan-based superparamagnetic iron oxide nanoparticles (CS-DX-SPIONs). Int J Nanomedicine 2018; 13: 1471-1482.

35. Shevtsov MA, Nikolaev BP, Ryzhov VA, Yakovleva LY, Dobrodumov AV, Marchenko YY, *et al.* Brain tumor magnetic targeting and biodistribution of superparamagnetic iron oxide nanoparticles linked with 70-kDa heat shock protein study by nonlinear longitudinal response. J Magn Magn Mater 2015; 388: 123-134.

36. Shevtsov MA, Nikolaev BP, Yakovleva LY, Marchenko YY, Dobrodumov AV, Mikhrina AL, *et al.* Superparamagnetic iron oxide nanoparticles conjugated with epidermal growth factor (SPION–EGF) for targeting brain tumors. Int J Nanomed 2014; 9: 273-287.

37. Davitt K, Babcock BD, Fenelus M, Poon CK, Sarkar A, Trivigno V, *et al.* The anti-cancer peptide, PNC-27, induces tumor cell necrosis of a poorly differentiated non-solid tissue human leukemia cell line that depends on expression of HDM-2 in the plasma membrane of these cells. Ann Clin Lab Sci 2014; 44: 241-248.

38. Sookraj KA, Bowne WB, Adler V, Sarafraz-Yazdi E, Michl J, Pincus MR. The anti-cancer peptide, PNC-27, induces tumor cell lysis as the intact peptide. Cancer Chemother Pharmacol 2010; 66: 325-331.

39. Zhao M, Beauregard DA, Loizou L, Davletov B, Brindle KM. Non-invasive detection of apoptosis using magnetic resonance imaging and a targeted contrast agent. Nat Med 2001; 7: 1241-1244.

40. Darban SA, Badiee A, Jaafari MR. PNC-27 anticancer peptide as targeting ligand significantly improved antitumor efficacy of Doxil in HDM2-expressing cells. Nanomedicine 2017; 12: 1475-1490.

41. Mokhtarzadeh A, Parhiz H, Hashemi M, Abnous K, Ramezani M. P53-derived peptides conjugation to PEI: an approach to producing versatile and highly efficient targeted gene delivery carriers into cancer cells. Expert Opin Drug Deliv 2016; 13: 477-491.

42. Rosal R, Pincus MR, Brandt-Rauf PW, Fine RL, Michl J, Wang H. NMR solution structure of a peptide from the mdm-2 binding domain of the p53 protein that is selectively cytotoxic to cancer cells. Biochemistry 2004; 43: 1854-1861.

43. Bychkova AV, Sorokina ON, Kovarski AL, Shapiro AB, Rosenfeld MA. The investigation of polyethyleneimine adsorption on magnetite nanoparticles by spin labels technique. Nanosci Nanotechnol Lett 2011; 3: 591-593.

44. Steitz B, Hofmann H, Kamau SW, Hassa PO, Hottiger MO, von Rechenberg B, *et al.* Characterization of PEI-coated superparamagnetic iron oxide nanoparticles for transfection: Size distribution, colloidal properties and DNA interaction. J Magn Magn Mater 2007; 311: 300-305.

45. Mulens-Arias V, Rojas JM, Sanz-Ortega L, Portilla Y, Pérez-Yagüe S, Barber DF. Polyethylenimine-coated superparamagnetic iron oxide nanoparticles impair *in vitro* and *in vivo* angiogenesis. Nanotechnol Biol Med 2019; 21: 102063.

46. He C, Hu Y, Yin L, Tang C, Yin C. Effects of particle size and surface charge on cellular uptake and biodistribution of polymeric nanoparticles. Biomaterials 2010; 31: 3657-3666.

47. National Center for Biotechnology Information (2022). PubChem Compound Summary for CID 122192877. Retrieved July 26, 2022 from https://pubchem.ncbi.nlm.nih.gov/compound/122192877.